




Article

# Impacts of Drought on Vegetation Assessed by Vegetation Indices and Meteorological Factors in Afghanistan

Iman Rousta <sup>1,2</sup>, Haraldur Olafsson <sup>3</sup>, Md Moniruzzaman <sup>4,5</sup>, Hao Zhang <sup>6</sup>, Yuei-An Liou <sup>7,\*</sup>, Terence Darlington Mushore <sup>8</sup> and Amitesh Gupta <sup>9</sup>

<sup>1</sup> Department of Geography, Yazd University, Yazd 8915818411, Iran; irousta@yazd.ac.ir

<sup>2</sup> Institute for Atmospheric Sciences-Weather and Climate, University of Iceland and Icelandic Meteorological Office (IMO), Bustadavegur 7, IS-108 Reykjavik, Iceland

<sup>3</sup> Institute for Atmospheric Sciences-Weather and Climate, Department of Physics, University of Iceland and Icelandic Meteorological Office (IMO), Bustadavegur 7, IS-108 Reykjavik, Iceland; haraldur68@gmail.com

<sup>4</sup> Center for Space Science and Technology in Asia and the Pacific (CSSTEAP), Dehradun 248001, India; moniruzzaman1313ku@gmail.com

<sup>5</sup> ASICT Division, Bangladesh Agricultural Research Institute, Gazipur 1701, Bangladesh

<sup>6</sup> Department of Environmental Science and Engineering Jiangwan campus, Fudan University, 2005 Songhu Road, Yangpu, Shanghai 200438, China; zhanghao\_fdu@fudan.edu.cn

<sup>7</sup> Center for Space and Remote Sensing Research (CSRSR), National Central University (NCU), Taoyuan 32001, Taiwan

<sup>8</sup> Department of Physics, Faculty of Science, University of Zimbabwe, MP167 Mt Pleasant, Harare 00263, Zimbabwe; tdmushore@science.uz.ac.zw

<sup>9</sup> Indian Institute of Remote Sensing, ISRO, Dehradun 248001, India; amitesh13gupta14@gmail.com

\* Correspondence: yueian@csrsr.ncu.edu.tw

Received: 11 June 2020; Accepted: 23 July 2020; Published: 29 July 2020



**Abstract:** Drought has severe impacts on human society and ecosystems. In this study, we used data acquired by the Moderate Resolution Imaging Spectroradiometer (MODIS) and Tropical Rainfall Measuring Mission (TRMM) sensors to examine the drought effects on vegetation in Afghanistan from 2001 to 2018. The MODIS data included the 16-day 250-m composites of the Normalized Difference Vegetation Index (NDVI) and the Vegetation Condition Index (VCI) with Land Surface Temperature (LST) images with 1 km resolution. The TRMM data were monthly rainfalls with 0.1-degree resolution. The relationship between drought and index-defined vegetation variation was examined by using time series, regression analysis, and anomaly calculation. The results showed that the vegetation coverage for the whole country, reaching the lowest levels of 6.2% and 5.5% were observed in drought years 2001 and 2008, respectively. However, there is a huge inter-regional variation in vegetation coverage in the study period with a significant rising trend in Helmand Watershed with  $R = 0.66$  ( $p$  value = 0.05). Based on VCI for the same two years (2001 and 2008), 84% and 72% of the country were subject to drought conditions, respectively. Coherently, TRMM data confirm that 2001 and 2008 were the least rainfall years of 108 and 251 mm, respectively. On the other hand, years 2009 and 2010 were registered with the largest vegetation coverage of 16.3% mainly due to lower annual LST than average LST of 14 degrees and partially due to their slightly higher annual rainfalls of 378 and 425 mm, respectively, than the historical average of 327 mm. Based on the derived VCI, 28% and 21% of the study area experienced drought conditions in 2009 and 2010, respectively. It is also found that correlations are relatively high between NDVI and VCI ( $r = 0.77$ ,  $p = 0.0002$ ), but slightly lower between NDVI and precipitation ( $r = 0.51$ ,  $p = 0.03$ ). In addition, LST played a key role in influencing the value of NDVI. However, both LST and precipitation must be considered together in order to properly capture the correlation between drought and NDVI.

**Keywords:** drought; Afghanistan; MODIS; NDVI; VCI; TRMM

---

## 1. Introduction

Drought has become one of the most frequent and critical natural disasters and hostile climatic phenomena that badly affect societies, water resources and ecosystem [1–4]. This has been evidenced as a causal factor in decreasing agricultural productivity [5]. The nature of drought is dynamic and causes difficulties in planning, monitoring, and prediction to assist drought-stricken areas [6,7]. Since the 1970s, numerous studies have used satellite-based land observations to monitor land surface dynamics [8–12]. Remotely sensed data provide a synoptic view of the land and a spatiotemporal context to measure drought impacts [9,13,14]. Geospatial techniques are used to derive various indices (vegetation, water content, and drought indices) for the effective analysis of drought using various image processing methods [15,16].

Remotely sensed drought indices are effective and suitable for spatial and temporal monitoring of drought conditions [17]. Different vegetation types can be clearly classified by using remote sensing vegetation indices, such as NDVI [18–20]. The indices for monitoring the intensity, impact, and duration of droughts include normalized difference vegetation index (NDVI), land surface temperature (LST), vegetation condition index (VCI), and temperature condition index (TCI), among other remote sensing-based drought indices [21]. NDVI is derived as the normalized difference in reflectance between the near-infrared (NIR) and visible red bands. It plays an important role in vegetation monitoring [22,23]. It measures the changes in chlorophyll content within the vegetation canopy so that higher NDVI values represent greater vigor and photosynthetic capacity of vegetation canopy [23–25]. The role of NDVI in vegetation dynamics, drought monitoring, and assessment has been frequently described during the last few decades [26–29]. NDVI has been calculated from the Advanced Very High-Resolution Radiometer (AVHRR) data from 1981 onwards. This creates a useful time-series data for monitoring vegetation dynamics all over the world [30]. Thereafter, for drought monitoring, NDVI is limited by the time lag between NDVI response and rainfall deficit [31–33]. The VCI has been found suitable for monitoring large scale response of vegetation to drought by numerous researchers, and its correlation with crop yield is strong [34–36]. However, these indices do not consider climatic factors such as variation in rainfall, especially in semi-arid regions where rainfall is a dominant factor [37]. Nowadays, drought and flood monitoring are also done by using remotely sensed precipitation produced by satellites, such as Tropical Rainfall Measuring Mission (TRMM), as an alternative to in-situ meteorological data [38–41]. Hence, the drought indices derived from remotely sensed data are developed by synthesizing precipitation and used for complex monitoring of drought [42].

Droughts are likely to be the norm by 2030, leading to land degradation and desertification in Afghanistan [43,44]. Some 80 percent of Afghans depend on rain-fed agriculture and cattle-grazing for their income, both of which are threatened by temperature increase and erratic rainfall [45]. It is estimated that 36 percent of people have been affected by natural disasters. The cumulative effects of more frequent and intense droughts on reservoirs and groundwater could threaten the water supply of entire communities in the most arid regions of Afghanistan, leading to a range of humanitarian crises, including disease, population displacement, and conflict [46]. Rising winter and spring temperatures will lead to a more rapid and earlier snowmelt, creating a risk of flash flooding. The impact of increasingly frequent flash floods is exacerbated by drought, which has the effect of hardening soils and reducing their permeability [47].

Afghanistan offers a variety of ecological conditions, meaning that different vegetation types cover the land surface. These vegetation types exhibit high biodiversity since the floristic influence from various neighboring regions is an important factor in floristic and vegetation patterns. Afghanistan lies at the “crossroad” of several biogeographical regions. While it is a very dry country, scarce rainfall varies by region and among lowlands and mountains. The country experiences a semi-arid and strongly

continental type of climate with major daytime and night-time temperature fluctuation. The eastern parts receive partly monsoonal rains in summer as the basis for the occurrence of various forest types that, however, are strongly degraded or deforested nowadays [48]. Vegetation all over Afghanistan has been severely influenced by human activities, and only a few high mountain and very dry desert areas retain a quasi-natural vegetation cover [49]. Desertification is a commonly known problem in most countries of the dry Middle East, Central Asia, and Afghanistan. In most parts, the vegetation depends on the winter rain, while in the south, winter rains are often irregular. Rainfall increases to the north and east resulting in better vegetation conditions in these parts. The eastern parts also receive some monsoon rains in summer [50]. Until recently, there are few studies on the relationship between climatological factors with drought and vegetation of Afghanistan, especially from a watershed point of view. In terms of ecological sustainability, Afghanistan is subject to deforestation, desertification, and severe soil erosion. Given that in this country, most of the watershed areas and their critical points are located in mountainous and hilly areas, these areas usually have very sparse or no tree cover. Studying vegetation dynamics and their link to drought in the region is very important to the ecological sustainability of this country.

It is fair to say that each environment has its own unique set of influential variables and complex characteristics, which must be properly accounted for when using different vegetation indices. Therefore, each vegetation index has its specific expression of green vegetation, its own suitability for specific uses, and some limitation factors. As for Afghanistan, it is a third world country that is absolutely lacking in sufficient in situ data for fostering the research of the current study's foci. Therefore, the authors must fully utilize their knowledge and experiences as well as searching the literature done in the field about vegetation indices to assess the vegetation variation in the country. Besides, the authors have attempted to apply some other parameters such as LST and TRMM to optimize more accurate findings about the vegetation variation in the study area.

The objective of this study is thus to investigate the relationship between vegetation coverage and drought stress in Afghanistan by using various indices, derived using MODIS, TRMM, and LST datasets. Is the precipitation alone dominating the drought occurrence? Should both precipitation and temperature be simultaneously considered? This study will answer the two questions and thus present: (a) the analysis of time-series database (2001 to 2018) of MODIS-derived NDVI and VCI; (b) the relationship between NDVI and VCI over Afghanistan; (c) the relationship between NDVI, precipitation and temperature (LST) over Afghanistan; (d) drought information provided by NDVI, VCI, SPI and LST, based on a seasonal comparison; and (e) investigation of drought conditions over Afghanistan.

## 2. Study Area and Material and Methods

### 2.1. Study Area

Afghanistan is located between latitudes of 29°30'–38°40' North and longitudes 60°30'–74°50' East, covering approximately 650,000 km<sup>2</sup> (Figure 1). The lowland plains in the south of Afghanistan experience extreme seasonal variations in temperature, with average summer (June to August) temperature exceeding 33 °C and mean temperature around 10 °C in winter (December to February). The majority of the country experiences very low temperatures all year round and is at high altitude. The highest region's average summer temperatures do not exceed 15 °C, while winter temperatures are below zero. Rainfall is very scarce in Afghanistan, with higher amounts received in the northern highlands starting in March and April. In the more arid lowlands, rainfall is rare and very unpredictable [49,51] (Figure 1). There are five major and distinct river basins defined in Afghanistan those are: the Amu Darya (ADW), Harirod-Murghab (HMW), Hilmand (HW), Kabul (KW) and Northern (NW) [52–54]. The ADW originates from the High Pamir Mountains of Afghanistan and Tajikistan and is surrounded in the north by the Ab-i Pamir River, and in the south by the Wakhan River. The ADW generates 57% of the total river flow in Afghanistan. The source of HMW is the western slope of the Koh-i Baba Mountains and Murghab (Tir Band-i Mountains in Turkistan). The HMW

contributes to a small 4% of the total annual flow in Afghanistan. The HW is the largest basin in Afghanistan which covers the southern half of the country, drain water from the Sia Koh Mountains in Hirat province to the eastern mountains in Gardez province and the Parwan Mountains northwest of Kabul. Though the HW shares about 43% of the national territory it drains only 11% of the total annual flow of Afghanistan. Starting from the Hindu Kush Mountains, the KW covers 700 km till flowing to the Indus River, Pakistan [55]. The KW shares 12% of the national territory, 23% of the total settlements, drains 26% of the total annual water flow, and nearly 35% of the total population of Afghanistan. The basin further divided in 3 major sub-basins based on its physiographic and hydro-climatic parameters those are Lower Kabul, Panjshir and Logar-Upper Kabul. The NW takes its sources in the high mountains of the central highlands and is the least annual flow contributing basin in Afghanistan by only 2% of the total (Figure 1).

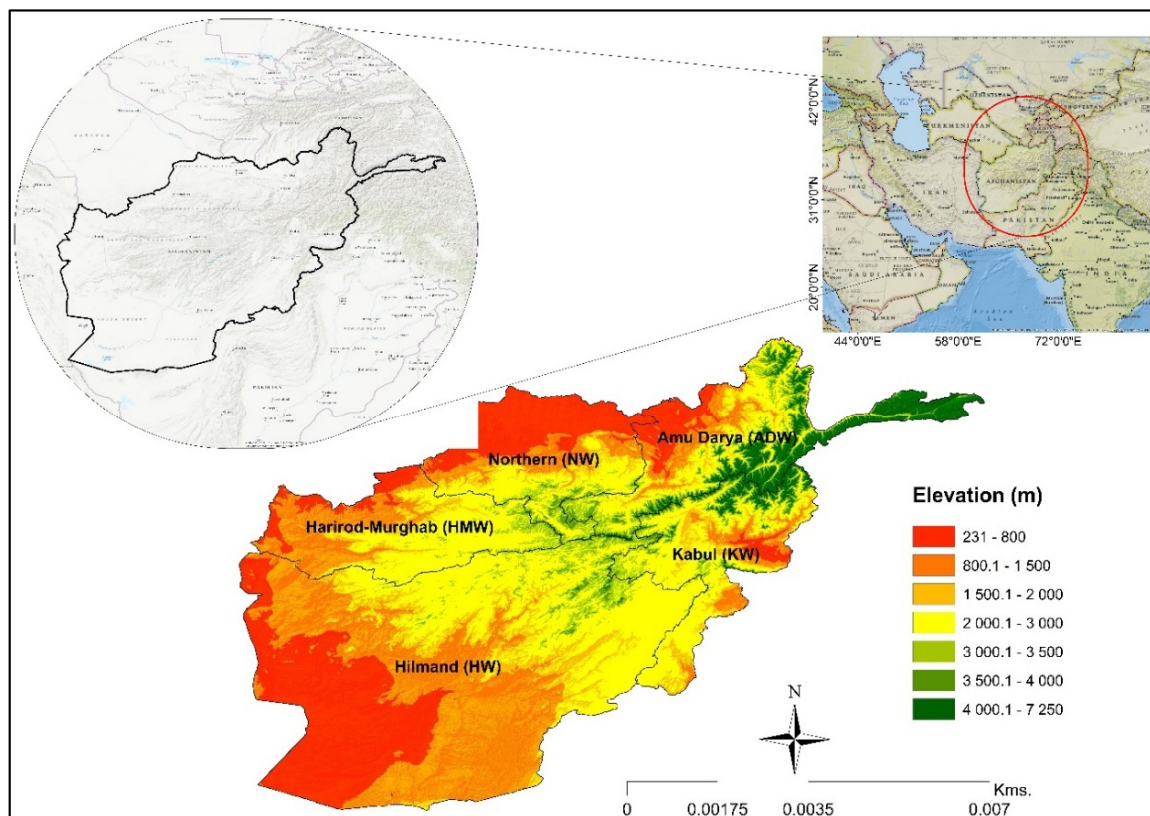


**Figure 1.** Elevation and the main watersheds of the study area, Afghanistan.

The great mass of vegetation is confined to the main ranges and their immediate offshoots, whilst it is almost entirely absent on the more distant and terminal prolongations. Vegetation all over Afghanistan has been severely influenced by human disturbance. Only a few high mountains and very dry desert areas retain a quasi-natural vegetation cover [49]. Desertification is a known long-term problem in most countries of the dry Middle East and Central Asia especially Afghanistan. In most parts, the vegetation depends on the winter rain, in the south, winter rains are often irregular. Rainfall increases to the north and east, resulting in better vegetation conditions in these parts. The eastern parts additionally receive some monsoon rains in summer [56] (Figure 2). The water systems for irrigation in Afghanistan can be classified into three major sources: (a) surface water as the main irrigation water source covering 86.5 percent of the irrigated area that can be clearly affected by precipitation variation, (b) springs accounting for 6.9 percent of the area, and (c) Karezes or Qanat for 6.2 percent with rest 0.4 percent from shallow and deep wells [57].

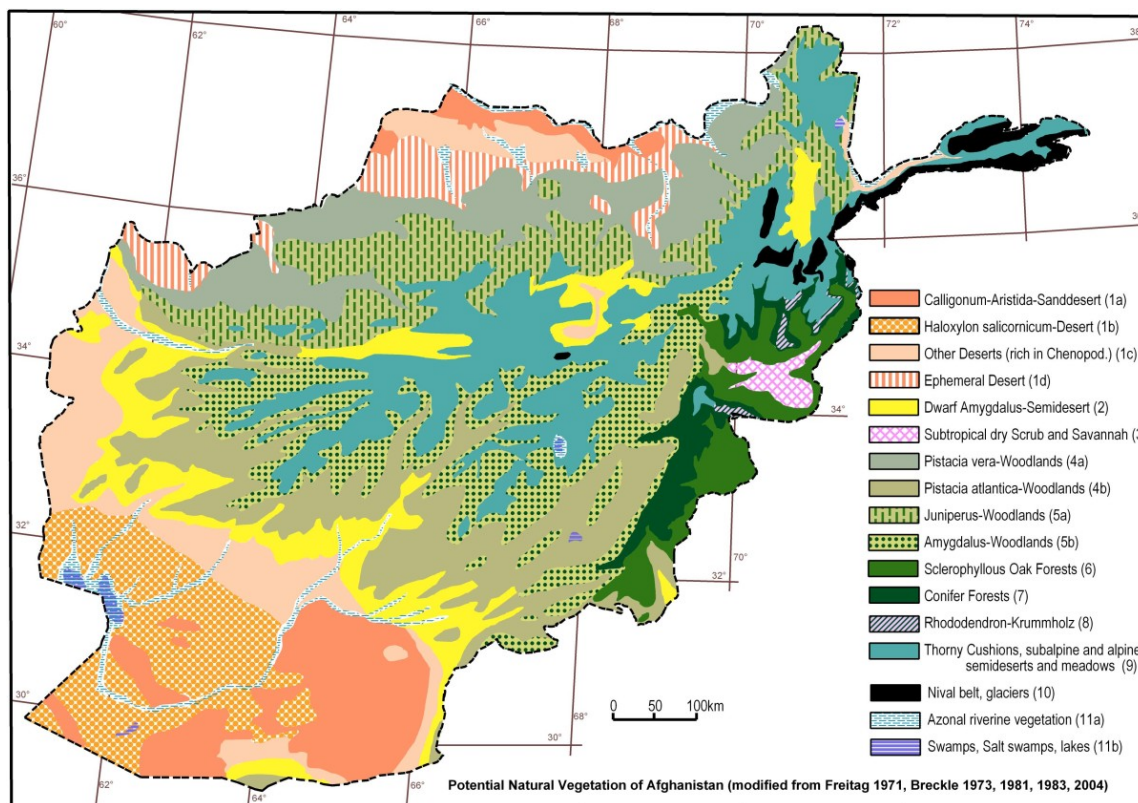


**Figure 2.** The natural vegetation of Afghanistan (adapted from [49]).

Afghanistan main vegetation types are shown in Figure 2 (natural vegetation of Afghanistan). They include: *Calligonum-Aristida*, sand desert (1a); *Haloxylon salicornicum*, desert (1b); other deserts (rich in chenopod) (1c); ephemeral desert (1d); dwarf *Amygdalus*, semidesert (2); subtropical dry scrub and savannah (3); *Pistacia vera*, woodlands (4a); *Pistacia atlantica*, woodlands (4b); *Juniperus*-woodlands (5a); *Amygdalus*, woodlands (5b); sclerophyllous oak forests (6); conifer forests (7); *Rhododendron-Krummholz* (8); thorny cushions, subalpine and alpine semi-deserts and meadows (9); nival belt, glaciers (10); azonal vegetation: riverine vegetation (11a); and azonal vegetation, swamps, salt swamps, lakes (11b) [49].

## 2.2. Data and Methodology

Remote sensing enables the collection of information from points, objects, and environmental phenomena by different sensors. It becomes one of the fundamental branches of science [9] to draw contextual drought scenarios in both spatial and temporal domains. This study used the Shuttle Radar Topography Mission (SRTM) digital elevation data with a resolution of 1 arc-second (~30 m) for providing the elevation map of the study area [58].

### 2.2.1. Normalized Difference Vegetation Index (NDVI)

The most common and useful index for investigating vegetation status is NDVI, which is measured with the leaf area index (LAI) and production pattern [15,59]. NDVI has been used by many scientists in different studies over the modern era [60–63]. The basic concept of NDVI is based on the fact that the internal mesophyll of healthy green leaves highly reflects near-infrared (NIR) radiation, whereas the leaf chlorophyll and other pigments absorb a large proportion of the red visible (RED) radiation [64]. This function of the internal leaf structure becomes reversed in case of unhealthy or water-stressed vegetation [15,30]. NDVI is calculated using Equation (1).

$$\text{NDVI} = \frac{\text{NIR} - \text{RED}}{\text{NIR} + \text{RED}} \quad (1)$$

The NDVI index ranges from  $-1$  to  $+1$  [65]. In this study, 437 images from Terra MODIS 16-day composite NDVI with 250-m resolution (MOD09Q1, collection v006) were downloaded by using Application for Extracting and Exploring Analysis Ready Samples (AppEEARS) software from <https://lpdaacsvc.cr.usgs.gov/appeears>, for 2001–2018 [66]. NDVI ranges from 0.2 and 1, corresponding to areas with greenness or plants. It should be above 0.5 for healthy and dense vegetation canopy, and fall within the range from 0.2 to 0.5 for the sparsely-vegetated areas [20]. In the current study, to calculate seasonal and yearly vegetation coverage, NDVI is divided to 8 categories (0.2–0.3, 0.3–0.4, 0.4–0.5, 0.5–0.6, 0.6–0.7, and 0.7–0.8), and the arithmetic mean was calculated for each pixel as Equations (2) to (6):

$$\text{Winter vegetation coverage} = \frac{\sum(\text{image 353 to image 065})}{6} \quad (2)$$

$$\text{Spring vegetation coverage} = \frac{\sum(\text{image 081 to image 161})}{6} \quad (3)$$

$$\text{Summer vegetation coverage} = \frac{\sum(\text{image 177 to image 257})}{6} \quad (4)$$

$$\text{Fall vegetation coverage} = \frac{\sum(\text{image 273 to image 337})}{5} \quad (5)$$

$$\text{Yearly vegetation coverage} = \frac{\sum(\text{image 017 to image 001})}{23} \quad (6)$$

### 2.2.2. TRMM

The TRMM was launched by NASA and the National Space Development Agency of Japan as a joint project [67,68]. It was developed to observe precipitation in tropical and subtropical regions. Its precipitation-related sensors include the visible and infrared radiometer system (VIRS), microwave imager (TMI), and precipitation radar (PR) [38,69]. TRMM data consists of three temporal resolution products of three-hourly (3B42), daily (3B42 derived), and monthly (3B43) extending from latitude  $50^\circ$  S to  $50^\circ$  N [70,71]. The Global Precipitation Climatology Center (GPCC) derives the TRMM monthly (3B43) dataset using Huffman's algorithm [72]. In this study, TRMM GPM\_3IMERGM monthly datasets from 2001 to 2018 used were acquired from Giovanni website (<https://giovanni.gsfc.nasa.gov/giovanni/>) with  $0.1 \times 0.1$  degrees spatial resolution [73]. The data was used for calculating the standardized precipitation index (SPI).

#### Standardized Precipitation Index (SPI)

McKee et al. (1993) developed the standardized precipitation index (SPI) to monitor drought [74], while Thom (1958) found the gamma distribution to fit climatological precipitation time, outlined by its frequency or chance density function:

$$f(x) = \frac{1}{\beta^\alpha \Gamma(\alpha)} x^{\beta-1} e^{-x/\beta} \quad (7)$$

where  $\alpha$  is a shape factor,  $\beta$  is a scale factor,  $x$  is equal to all non-zero values in the precipitation history. It is assumed,  $\alpha > 0$  and  $\beta > 0$ . The gamma function may be expressed as follows:

$$\Gamma(\alpha) = \int_0^\infty e^{-t} t^{\alpha-1} dt \tag{8}$$

where  $\Gamma(\alpha)$  is the gamma function.

SPI calculation includes fitting a gamma probability density function for a station to a given frequency distribution of overall precipitation. The maximum likelihood solutions are used to optimally estimate  $\alpha$  and  $\beta$  as follows [75],

$$\hat{\alpha} = \frac{1}{4A} \left( 1 + \sqrt{1 + \frac{4A}{3}} \right) \tag{9}$$

$$\hat{\beta} = \frac{\bar{x}}{\alpha} \tag{10}$$

$$A = \ln \bar{x} - \frac{\sum \ln(x)}{n} \tag{11}$$

where  $n$  is number of precipitation observations,  $A$  is a measure of the skewness of the distribution  $\bar{x}$  is the arithmetic mean of all non-zero values. The cumulative probability is given by:

$$G(x) = \int_0^x g(x) dx = \frac{1}{\beta^\alpha \tau^\alpha} \int_0^x x^{\alpha-1} e^{-x/\beta} dx \tag{12}$$

where  $t = x/\beta$ ; and  $G(x) = \frac{1}{\Gamma(\alpha)} \int_0^x t^{\alpha-1} e^{-t} dt$ .

The gamma function is undefined for  $x = 0$ , and a precipitation distribution may contain zeros. The cumulative probability becomes

$$H(x) = q + (1 - q) G(x) \tag{13}$$

The value of  $q$  is assumed to be a probability of zero. If  $m$  is the number of zeros in a precipitation time series, according to Thom (1958)  $q$  can be estimated by  $m/n$ . The cumulative probability,  $H(x)$ , is then transformed to the standard normal random variable  $Z$  with mean zero and variance of one, which is the value of the SPI [75]. SPI is categorized based on the range of values shown in Table 1.

**Table 1.** Wet and drought period classification according to the SPI index [76,77].

Index Value	Class	Description
Non Drought	$SPI \geq 2.00$	Extremely wet
	$1.50 \leq SPI < 2.00$	Very wet
	$1.00 \leq SPI < 1.50$	Moderately wet
	$-1.00 \leq SPI < 1.00$	Near normal
Drought	$-1.50 \leq SPI < -1.00$	Moderate drought
	$-2.00 \leq SPI < -1.50$	Severe drought
	$SPI < -2.00$	Extreme drought

### 2.2.3. Land Surface Temperature (LST)

In this study, for calculating the daytime LST, we used 828 images of the sixth product, MOD11A2, an eight-day LST product by averaging from two to eight days of the MOD11A1 (MOD11A2.006\_LST\_Day\_1km). The product was downloaded by using Application for Extracting and Exploring Analysis Ready Samples (AppEEARS) software from <https://lpdaacsvc.cr.usgs.gov/appears>, for 2001 to 2018 [66]. To calculate yearly LST the arithmetic mean has been calculated for each pixel as Equation (14).

$$\text{Yearly LST} = \frac{\sum(\text{image 009 to image 001})}{46} \tag{14}$$

#### 2.2.4. Vegetation Condition Index (VCI)

The vegetation condition index (VCI) was first introduced by Kogan (1995, 1997) [26,78]. It effectively shows how close the current month's NDVI is to the minimum NDVI calculated from the long-term record of remote sensing data [79]. The VCI is a pixel-based normalization of the NDVI to separate the long-term ecosystem changes from the short-term weather-related NDVI fluctuation and reflects relative changes in the vegetation condition from extremely bad to optimal [34,42]. The VCI is a better indicator of drought stress impact on vegetation condition than NDVI. It ranges from 0 (extremely unfavorable) to 1 (optimal). It is close or equal to 0 in an extremely dry month when the vegetation condition is poor. Fair vegetation conditions are reflected by a VCI of 0.5, while VCI is close to 1 when vegetation is in the best state [80]. It is obtained by the following formula:

$$VCI = \left( \frac{NDVI - NDVI_{min}}{NDVI_{max} - NDVI_{min}} \right) \times 100 \quad (15)$$

where NDVI is the smoothed pixel values of NDVI based on the Savitzky–Golay filter [81].  $NDVI_{max}$  and  $NDVI_{min}$  are respectively maximum NDVI and minimum NDVI, calculated by the corresponding pixels in monthly, seasonal, and yearly period from the entire NDVI records for the whole study area from 2001 to 2018.

#### 2.2.5. Linear Regression

This study used the linear regression to define the correlations, at a significance level of 0.05, for further analysis. Linear regression is a statistical method to model the relationship between two variables by fitting a linear equation to observed data. One variable is considered to be an explanatory variable, and the other is considered to be a dependent variable [82]. A linear regression model can be described as follows:

$$y_i = a + bx_i \quad (16)$$

where  $a$  and  $b$  are regression coefficients. The coefficients of (11) can be obtained from the given  $(x_i, y_i)$ .

### 3. Results and discussion

#### 3.1. NDVI Change

Figure 3 shows the average vegetation coverage in the study area during the whole study period. This figure reveals that the NDVI gradually rose from the first of January (with 8% of the study area), and the rise was continuously seen rapidly until late April and the first of May with about 20% of the area (about 132,000 km<sup>2</sup>). From the tenth of May, the vegetation coverage gradually decreased, and the coverage reached its minimum yearly coverage at the mid of October with 6% vegetation coverage (about 37,500 km<sup>2</sup>). The vegetation coverage experienced a very weak rise from late November to middle December, and then a falling trend was observed. Accordingly, the main growing season in Afghanistan starts around the first of January and ends in the first ten days of May (Figure 3).

The annual variation rates of the different types of NDVI coverage (0.2–0.3, 0.3–0.4, 0.4–0.5, 0.5–0.6 and >0.6) were calculated for each pixel for the study area by multiplying the number of pixels with different NDVI values (0.2–0.3, ...) to the area of each pixel (62,500 m<sup>2</sup>) between 2001 and 2018. The temporal trend of annual NDVI coverage showed heterogeneity in the study area. Two types of vegetation (NDVI 0.2–0.4) show no trend, and the other types of vegetation (0.41–0.8) show a significant increasing trend. Figure 4 shows the temporal trends of the annual coverage of NDVI in the area.

Figures 5 and 6 show the relationship between annual vegetation coverage (drought severity) determined by using NDVI and VCI index in Afghanistan during the study period (2001 to 2018). The drought area (DA) and no drought area (NDA) are defined as the areas with a VCI index between 0 and 50% (DA), and between 50.1 and 100% (NDA), respectively. For the whole of Afghanistan (about 650,000 km<sup>2</sup>) in the study period, on average, 11.66% has been covered by vegetation (75,800 km<sup>2</sup>).



There were some years with the maximum and minimum of DA in the study area as years 2001, and 2008 with maximum DA (84 and 72% of the study area, respectively), and years 2010, and 2016 with the lowest value of DA (21.4 and 22.5% of the study area, respectively). The vegetation coverage of those years also has been respectively among the maximum and minimum in the study period (2001 with 6%, 2008 with 5.4%, 2010 with 16.3% and 2016 with 14.9% of the study area). As shown, there is a significant relationship between DA and NDA with NDVI coverage in the study area, while the trends of the NDVI, DA, and NDA were temporally coherent, as indicated with the regression models of the DA versus NDVI ( $r = 0.77, p < 0.05$ ) and the NDA versus NDVI ( $r = 0.77, p < 0.05$ ) (Figures 5 and 6).

Table 2 shows the area covered by each class of NDVI in the study area. It indicates that 70.2% of all of the vegetation in Afghanistan was in the NDVI range of 0.2–0.3, NDVI range of 0.3–0.6 was 29.4%, and NDVI >0.6 was just less than 0.5% of the vegetation (Table 2 and Figure 7). Figure 7 shows the area of Afghanistan with different categories of NDVI between 2001 to 2018. It is clearly observable that Afghanistan is rather sparsely vegetated. Furthermore, only 29.9% of the country is vegetated with NDVI higher than 0.3. Obviously, Afghanistan demonstrates the characteristics of an arid and semi-arid climate.

**Table 2.** The area covered by different NDVI categories (km<sup>2</sup>) in Afghanistan between 2001 and 2018.

Year	NDVI 0.2–0.3	NDVI 0.3–0.4	NDVI 0.4–0.5	NDVI 0.5–0.6	NDVI 0.6–0.7	NDVI 0.7–0.8
2001	25,036	9613	3712	1320	321	7
2002	57,744	14,884	4235	1189	177	2
2003	72,583	24,661	4323	1049	108	0
2004	64,816	13,560	3630	965	135	0
2005	63,457	13,476	4218	833	61	0
2006	39,943	12,282	3896	871	92	0
2007	57,467	17,498	4120	954	120	2
2008	20,916	9978	3431	972	156	3
2009	75,356	23,642	5944	1090	131	2
2010	80,358	17,998	5545	1544	287	3
2011	36,993	12,657	4543	1307	177	1
2012	55,481	14,436	4246	1096	120	0
2013	65,988	15,982	6135	1377	208	4
2014	47,301	13,978	5699	1624	307	12
2015	69,112	19,007	7038	1810	400	13
2016	71,390	15,998	6642	1992	549	48
2017	44,531	14,097	6141	1517	219	4
2018	37,759	14,656	7531	2293	672	55
Average	54,791	15,467	5057	1322	236	9

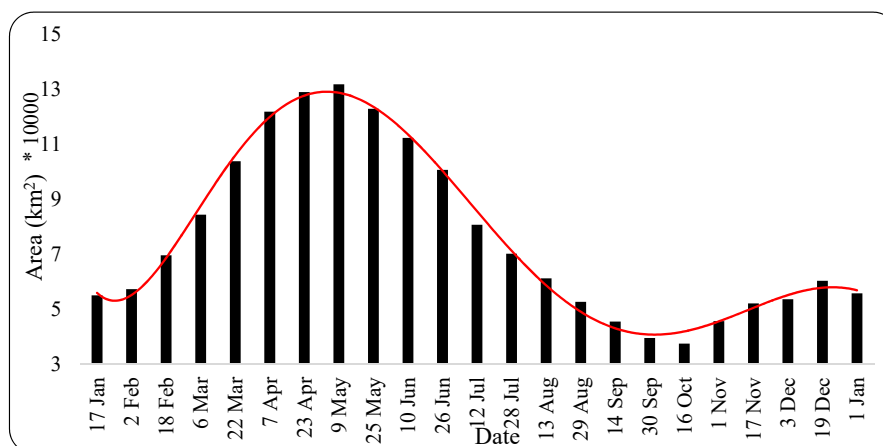


**Figure 3.** The average vegetation coverage in Afghanistan between 2001 and 2018.

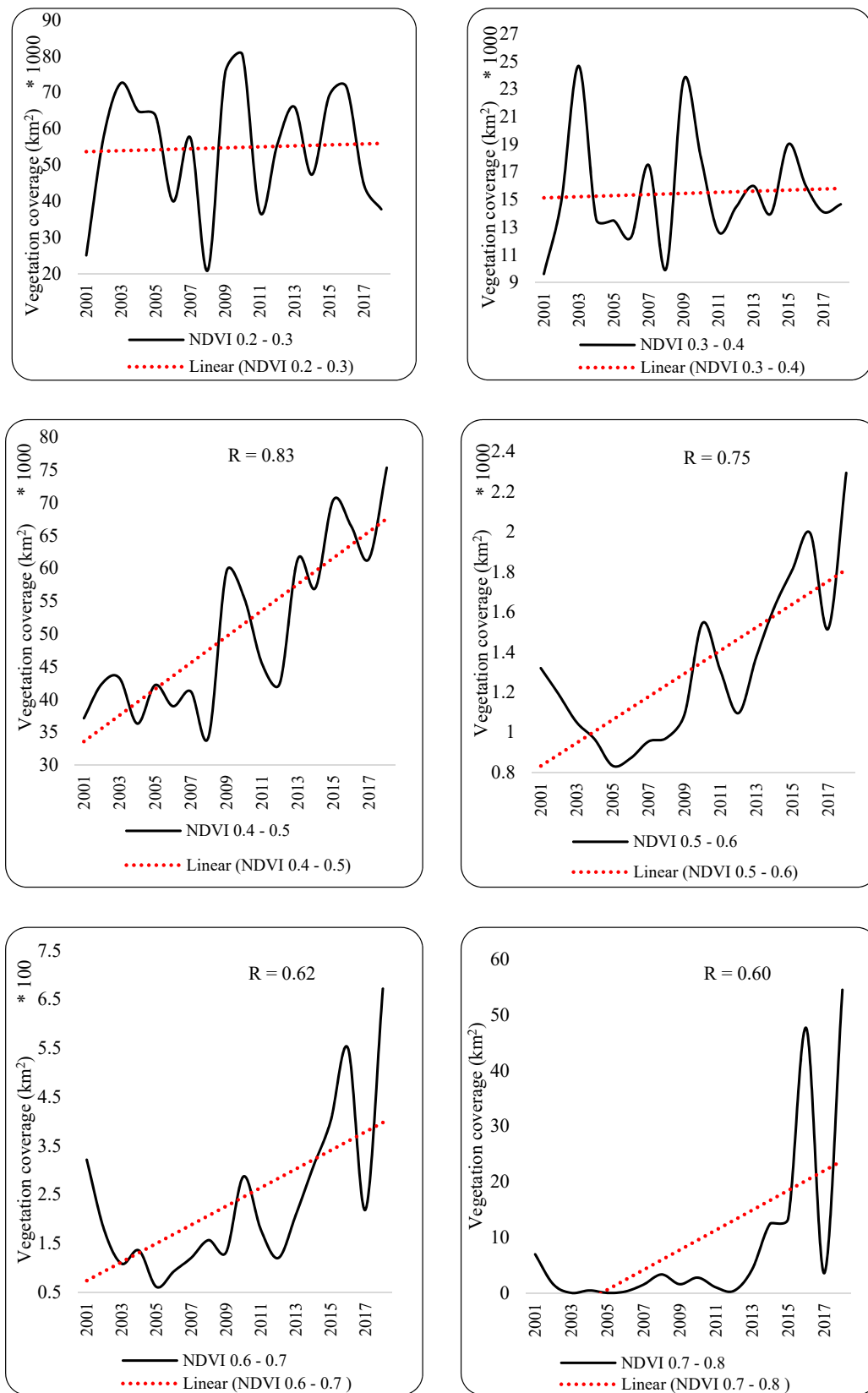


**Figure 4.** Time series of different categories of NDVI for the study area between 2001 and 2018 (significance level at  $p = 0.05$ ).

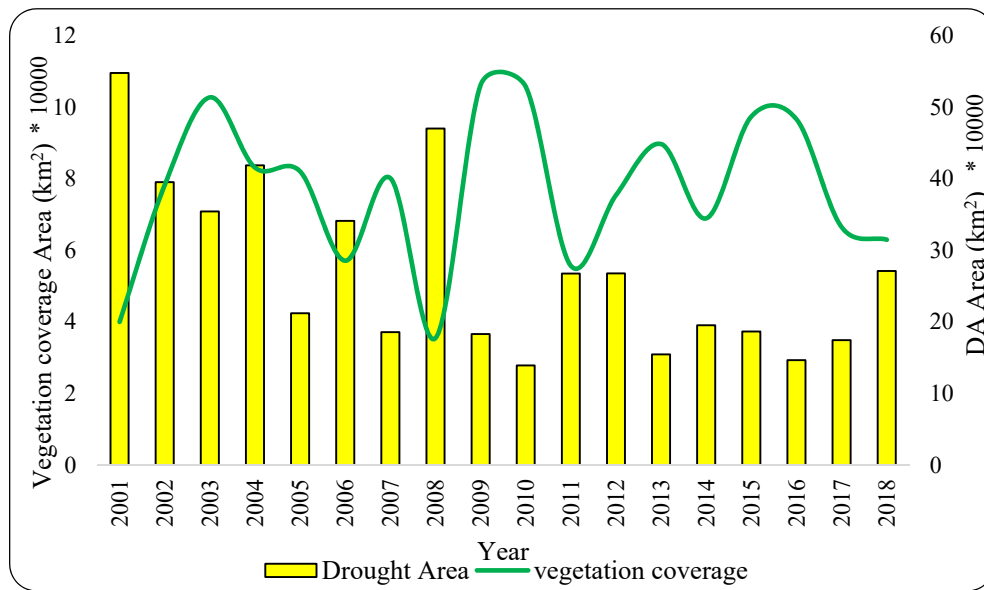


Figure 5. The relationship between vegetation coverage area and areas of DA and NDA in Afghanistan between 2001 and 2018.

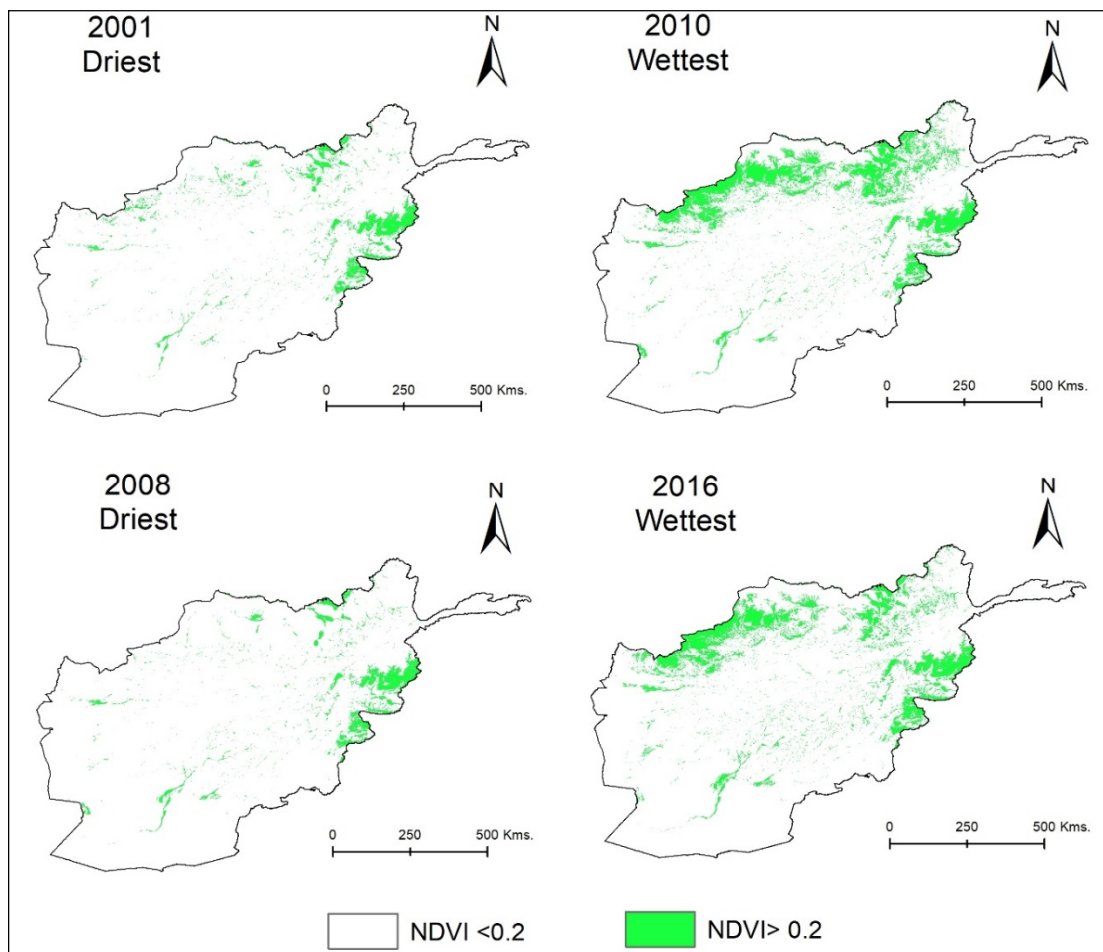


Figure 6. Annual mean NDVI for the driest and wettest years in Afghanistan between 2001 and 2018.

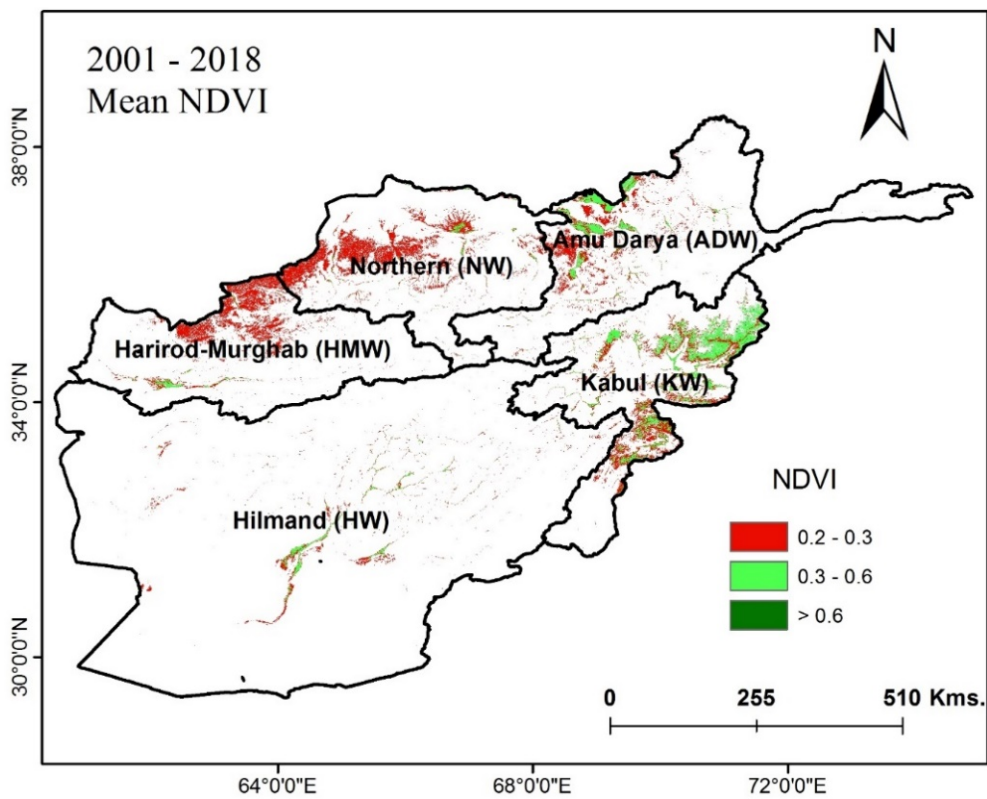


Figure 7. Area of Afghanistan with different categories of NDVI between 2001 and 2018.

Table 3 shows the correlation between DA (VCI 0–50%) with spatial coverage of each NDVI class in the study period. There exists a meaningful negative relationship between NDVI 0.2–0.3 categories with DA and an insignificant negative relationship between NDVI 0.6–0.8 categories with DA. The table shows that the dense and semi-dense vegetation (NDVI > 0.5) are less sensitive to drought condition than the sparse vegetation (NDVI 0.2–0.5). Because the dense vegetation can endure a short-term drought (one or two years), the sparse vegetation cannot withstand even a seasonal drought. It cannot be concluded from the relationship between DA condition, with all categories of NDVI, that it is just precipitation to control the vegetation variation. Hence, it is needed to study the seasonal relationship between VCI and NDVI.

Table 3. The correlation between DA with spatial coverage of different NDVI categories in Afghanistan between 2001 and 2018.

	NDVI 0.2–0.3	NDVI 0.3–0.4	NDVI 0.4–0.5	NDVI 0.5–0.6	NDVI 0.6–0.7	NDVI 0.7–0.8
DA	−0.59 *	−0.46 *	−0.68 *	−0.37	−0.19	−0.21

Note: \* denotes significance level at  $p = 0.05$ .

### 3.2. Watershed NDVI Variation

Figure 8 shows the time series and vegetation coverage of each watershed in the study area between 2001 and 2018. NW and ADW watershed share 27% and 23% of the vegetation coverage of the country, respectively. In contrast, KW, HMW, and HW share 22%, 19%, and 9% of the whole country’s vegetation, respectively.

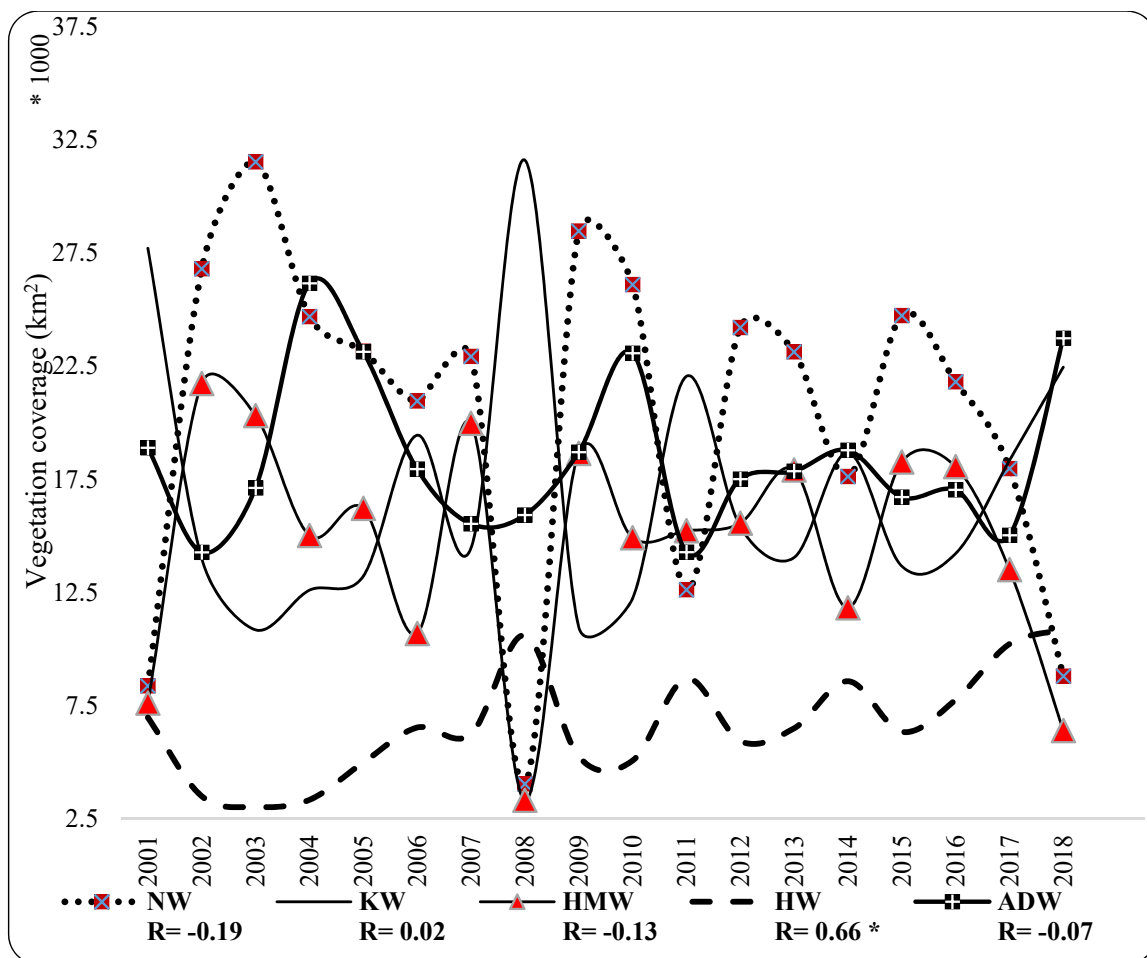


**Figure 8.** Time series and trend of vegetation coverage of each watershed in Afghanistan between 2001 and 2018 (\* denotes significance level at  $p = 0.05$ ).

In the study period, there was a significantly positive rising trend in vegetation coverage in HW with  $R = 0.66$  ( $p$  value = 0.05). The other watersheds do not exhibit a significant trend, but a negative falling trend was observed in HMW and NW. Also, the figure shows the inter-regional and interannual vegetation coverage for the five main watersheds in the study area between 2001 and 2018. Note that there is a different attitude between the main watersheds, especially KW and HW watersheds that are influenced by Indian Monsoon (Figure 8). On the other hand, KW and HW located in the Eastern and Southern parts of the country are affected by the monsoon from the Indian sub-continent [57].

Table 4 shows the correlation between vegetation coverage of the five main watersheds with each other in Afghanistan. The highest positive correlations were found in the two pairs HMW and NW, and HW and KW with  $R = 0.87$  and  $0.73$ , respectively. In contrast, the negative correlations were clearly observable between KW and NW with  $R = -0.93$ , between HMW and KW with  $R = -0.87$ , between HW and NW with  $R = -0.82$ , and between HMW and HW with  $R = -0.69$ . Finally, it can be concluded that the vegetation coverages of different watersheds in Afghanistan are affected by three main different atmospheric patterns (one pattern for KW and HW, one for HMW and NW, and the other one for ADW watershed (Table 4).

**Table 4.** The correlation matrix of time series of vegetation coverages between five watersheds in the study area between 2001 and 2018.

Watersheds	NW	KW	HMW	HW	ADW
NW	1				
KW	−0.96 *	1			
HMW	0.87 *	−0.87 *	1		
HW	−0.82 *	0.73 *	−0.69 *	1	
ADW	0.06	−0.19	−0.23	−0.21	1

Note: \* denotes significant at  $p = 0.05$ .

Table 5 shows the correlation between seasonal DA with seasonal spatial coverage of each NDVI class in the study period. It shows that there is a negative correlation between NDVI coverage with DA in all of seasons. However, the correlation is more in the warm seasons (spring and summer) than the cool seasons (winter and fall). The correlation is significant just in summer season and just for NDVI 0.4–0.7 (respectively,  $R = -0.47, -0.50$  and  $-0.46$ ,  $p$  value = 0.05), but the correlation between all NDVI categories with DA is more negative in the summer season than the other seasons. This is because the LST is high enough for the plants to grow in the warm seasons. That is, if there is enough water, the plants grow naturally. In contrast, if there is insufficient water, the plants will experience pressure to high LST (Table 5).

**Table 5.** The correlation between seasonal DA with seasonal spatial coverage of different NDVI categories in Afghanistan between 2001 and 2018.

	NDVI 0.2–0.3	NDVI 0.3–0.4	NDVI 0.4–0.5	NDVI 0.5–0.6	NDVI 0.6–0.7	NDVI 0.7–0.8
WINTER	−0.22	−0.25	−0.14	−0.02	0.01	−0.07
SPRING	−0.37	−0.40	−0.29	−0.25	−0.24	−0.22
SUMMER	−0.40	−0.40	−0.47 *	−0.50 *	−0.46 *	−0.38
FALL	−0.24	−0.29	−0.26	−0.22	−0.21	−0.18

Note: \* denotes significant at  $p = 0.05$ .

### 3.3. Relationship Between NDVI with Precipitation and LST

Figure 9 shows the relationship between yearly NDVI coverage with annual precipitation and LST in Afghanistan. It is observed that there is a significant correlation between NDVI with precipitation ( $p = 0.03$ ,  $r = 0.51$ ) and an insignificant relationship between NDVI with LST ( $p = 0.55$ ,  $r = 0.15$ ). The years 2001, 2002, 2008, and 2017 had the minimum precipitation (107.7, 219.8, 250.6, and 203.4 mm, respectively), and years 2012, 2013, 2014, and 2015 had the maximum precipitation (511, 536.3, 548.2 and 692.2 mm, respectively). The agricultural sector is highly vulnerable to changes in rainfall patterns, increased LST, and snowmelt. Agricultural productivity and crop choice availability are impacted by reduced river flow from earlier snowmelt, increased soil evaporation, and less frequent rain during peak cultivation seasons [47]. The harmony between the driest years with NDVI coverage is clear in the years 2001 and 2008, but not obvious in the years 2002 and 2017, which, despite the drought, experienced an increase in NDVI coverage. Also, the years 2001, 2013, 2016, and 2017 were the hottest years (20, 19.7, 20.3, and 19.8 °C, respectively) and years 2008, 2009, 2010, and 2018 (18.17, 17.07, 17.82, and 17.08 °C, respectively) were the coldest years. It can be concluded that the LST by controlling the soil moisture has a key role in increasing/decreasing trend of NDVI coverage in the study area. For example, in the year 2001 because of low SPI and high LST, it was one of the lowest coverages of NDVI (40,010 km<sup>2</sup>), due to decreasing soil moisture in relation to high LST and water scarcity as a result of low precipitation. On the other hand, in the year 2008, because both LST and SPI were lower than normal value, the least NDVI coverage occurred (35,457 km<sup>2</sup>). The year 2008, as the driest (less vegetation coverage) year, is the last year of a period of 8 dry years with precipitation lower than normal. Therefore, it was clearly observed that, after a long continuous period (8 years) with drought

conditions, all types of vegetation coverage had been affected, and finally, the year 2008 was the driest during the study period. On the other hand, a drought occurred in the year 2017 after five wet years during the study period. Hence, despite with LST higher than normal and precipitation lower than normal, both of them can cause a stressful situation for vegetation coverage. However, due to the facts of existing sufficient water supplies, having enough surface and ground waters, as well as the development of irrigation areas, the year had a normal situation in vegetation coverage. In 2009 and 2010, despite that the precipitation was tightly near the historical normal, the NDVI coverage was the highest in the study period because the LST was below normal. In contrast, even in the years 2014 and 2015, which were the wettest years in the study period, NDVI coverage could not reach the highest level because of low LST (Figure 9).

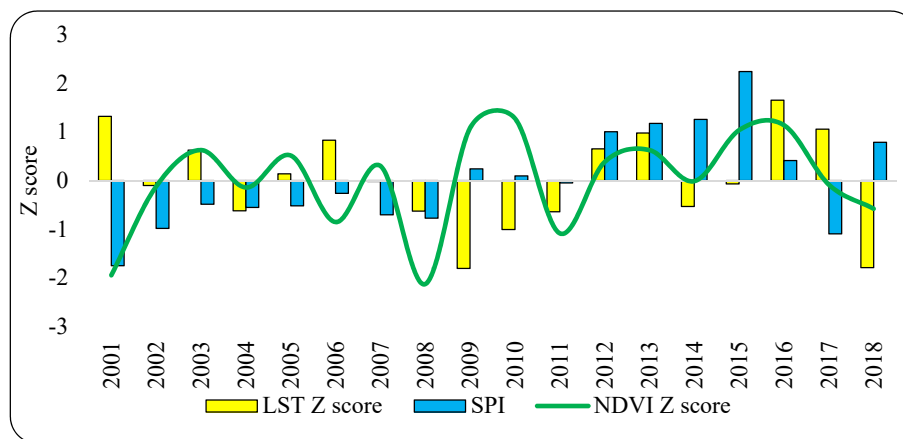


**Figure 9.** The relationship between anomaly of yearly vegetation coverage with the anomaly of annual precipitation and LST in Afghanistan between 2001 and 2018.

The average annual LST of Afghanistan in the study period did not show an obvious trend, while precipitation showed an insignificant increasing trend. The increasing trend from the year 2009 was more sensible. It was observed that from the year 2009, there were no decreases in NDVI coverage in the study area due to precipitation shortage (Figure 9). According to climatic norms used by the World Meteorological Organization (WMO), the mean annual temperature has increased by 0.6 °C since 1960, at an average rate of around 0.13 °C per decade. Mean rainfall over Afghanistan has slightly decreased at an average rate of 0.5 mm per month (or 2% per decade) since 1960 [47]. It can be said that in arid and semi-arid areas, like almost part of the Middle East, vegetation coverage does not depend on just either precipitation or LST. However, either precipitation or LST alone can have a strengthening or weakening effect on the vegetation coverage. Therefore, it is very important to consider both LST and precipitation for analyzing the variations in the vegetation coverage in these regions.

#### 3.4. Watershed Vegetation Coverage and Precipitation

Figure 10 shows the relationship between vegetation coverage and precipitation in the study area between 2001 and 2018. It demonstrated that there was no significant correlation between vegetation coverage and precipitation. Also, the correlation was found to be near zero ( $R = -0.02$ ) in HMW, while positive correlations were observed in NW, HW, and ADW with  $R = 0.27$ ,  $0.36$ , and  $0.17$ , respectively, and negative correlation was seen in KW with  $R = -0.28$ . Thus, it seems that, in these regions, vegetation coverage cannot be predicted just by using the precipitation, as further illustrated in Figure 8. This finding is not completely the same as that found by Ji and Peters [33]; vegetation greenness can be predicted using current and antecedent precipitation. Such inconsistent findings are a result of the fact that the previous research [34] did not consider temperature as an influencing factor in their study. That is, temperature plays an important role to alter the vegetation pattern in the semi-arid and arid regions, such as middle east and Afghanistan.

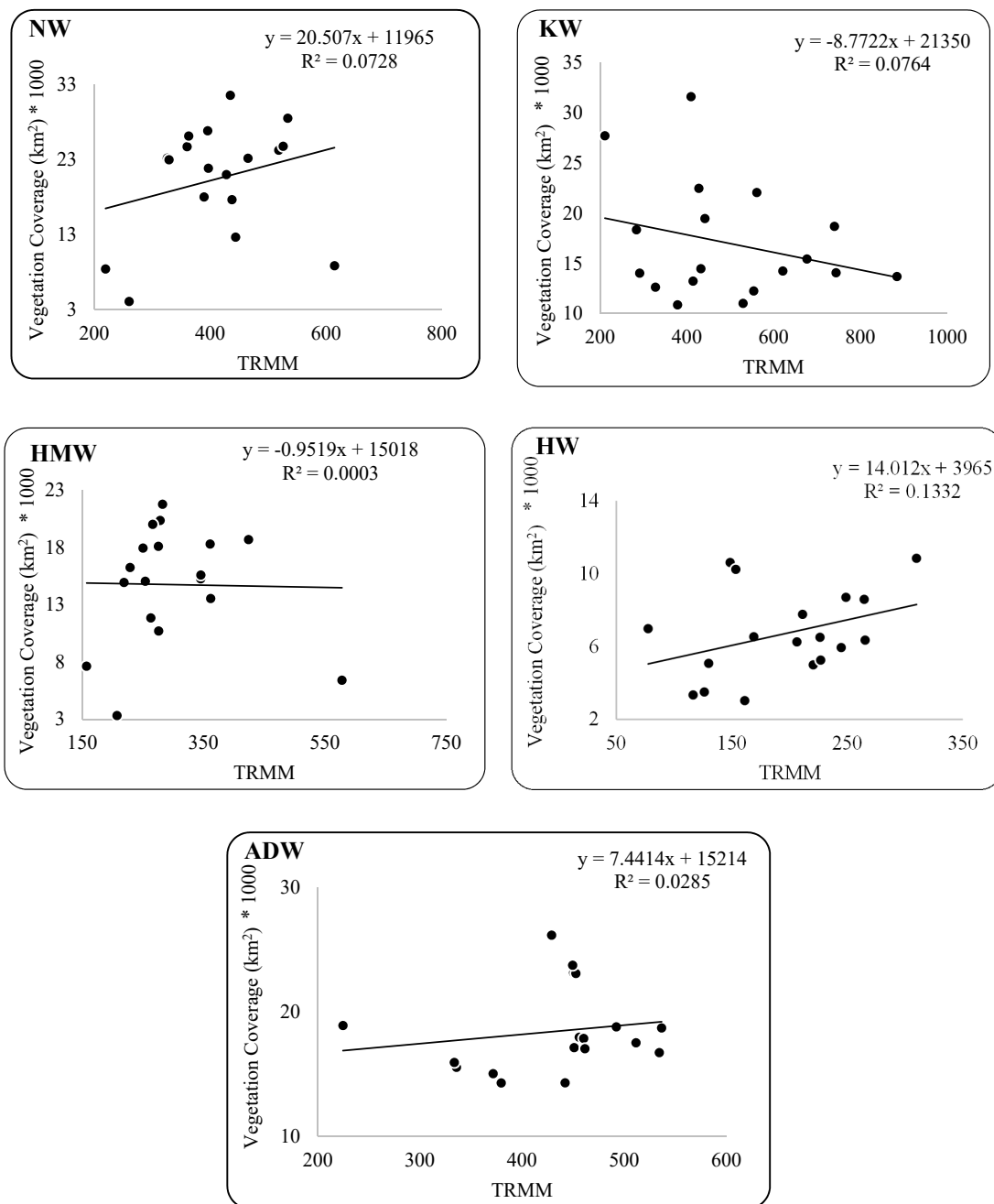


**Figure 10.** Scatter plot of time series of precipitation and vegetation coverage of each watershed in Afghanistan between 2001 and 2018.

#### 4. Conclusions

The present study attempted to identify drought years over Afghanistan using remotely sensed data and to identify the best indicators for studying vegetation coverage in the study area. It was found that MODIS NDVI-derived VCI with precipitation and LST images can be useful for monitoring of drought in Afghanistan. There was an increased rate of annual NDVI coverage ranging from 0.2–0.3 to 0.5–0.8 for the whole study area. There was a significant relationship between the VCI and NDVI coverage in the study area, while the regression between DA with NDVI and for the NDA with NDVI has been the same ( $r = 0.77$ ,  $p = 0.0002$ ). The relationship was negative between all NDVI categories with extreme, and moderate drought conditions, and meaningful positive relationships between all NDVI



categories with extreme, severe, moderate, and light wet conditions were obtained. The relationship between severe droughts and NDVI was negatively significant in categories (NDVI 0.2–0.4 and 0.6–0.8). In the study period, the seasonal NDVI coverage well agreed with seasonal VCI, but such trends in spring and summer were more sensible than those during winter and fall seasons.

There was a significant correlation between NDVI and precipitation and an insignificant relationship between NDVI and LST. It seemed that LST had a key role in modifying NDVI coverage. Years with nominal precipitation, having an average LST lower than normal years, benefit vegetation growth due to low evapotranspiration. A year with high precipitation and very low LST resulted in suppressed vegetation growth and lower coverage of high NDVI values. The least vegetation coverage was found in the years 2001 and 2008, while the most vegetation coverage was found in the years 2010 and 2016. Such finding is consistent with those found by Pervaz et al. [83]. The vegetation coverage of different watersheds in Afghanistan was affected by three main atmospheric patterns (one pattern for KW and HW, one for HMW and NW, and the other one for ADW). Such findings are consistent with that found by Shokory et al. [84].

In arid and semi-arid regions such as Afghanistan, the lag time between precipitation variation and vegetation coverage is primarily controlled by LST. In these regions, it cannot be doable to predict the vegetation coverage just by using the precipitation variation, while this result is not completely consistent with the findings of Ji and Peters [33]; this gives space for further research.

The average annual LST of Afghanistan in the study period did not show any trend, while precipitation showed an insignificant increasing trend. The response of vegetation to an increasing trend of precipitation was sensible from the year 2009. Finally, it can be concluded that, with the currently increasing trend in precipitation, especially from the year 2009, and with no recognized trend in LST in the study period, vegetation in Afghanistan will not be decreased in the near future. However, the conclusion did not consider other factors, such as the political situation in the country, which could affect water and vegetation management.

**Author Contributions:** I.R., M.M. and H.Z. proposed the topic. The authors, I.R., H.O., M.M., H.Z., Y.-A.L., T.D.M. and A.G. commanded the data processing, analysis, and wrote the manuscript. I.R., H.O., M.M., H.Z., Y.-A.L., T.D.M. and A.G. helped to enhance the research design, analysis, interpretation, and manuscript writing. Y.-A.L. finalized the manuscript. All authors have read and agreed to the published version of the manuscript.

**Funding:** Y.A.L. appreciates the financial support from MOST of Taiwan under the codes 108–2111-M-008-036-MY2 and 108–2923-M-008-002-MY3.

**Acknowledgments:** Iman Rosta is deeply grateful to his supervisor (Haraldur Ólafsson, Professor of Atmospheric Sciences, Institute for Atmospheric Sciences-Weather and Climate, and Department of Physics, University of Iceland and Icelandic Meteorological Office (IMO)), for his great support, kind guidance, and encouragement.

**Conflicts of Interest:** The authors declare no conflict of interest.

## References

1. Bhuiyan, C.; Singh, R.; Kogan, F. Monitoring drought dynamics in the Aravalli region (India) using different indices based on ground and remote sensing data. *Int. J. Appl. Earth Obs. Geoinf.* **2006**, *8*, 289–302. [[CrossRef](#)]
2. Zhang, N.; Hong, Y.; Qin, Q.; Zhu, L. Evaluation of the visible and shortwave infrared drought index in China. *Int. J. Disaster Risk Sci.* **2013**, *4*, 68–76. [[CrossRef](#)]
3. Rosta, I.; Nasserzadeh, M.; Jalali, M.; Haghghi, E.; Ólafsson, H.; Ashrafi, S.; Doostkamian, M.; Ghasemi, A. Decadal spatial-temporal variations in the spatial pattern of anomalies of extreme precipitation thresholds (case study: Northwest Iran). *Atmosphere* **2017**, *8*, 135. [[CrossRef](#)]
4. Dorjsuren, M.; Liou, Y.-A.; Cheng, C.-H. Time series MODIS and in situ data analysis for Mongolia drought. *Remote Sens.* **2016**, *8*, 509. [[CrossRef](#)]
5. Denli, H.H.; Denli, G.O. The use of soil and water resources at the Mediterranean region in Turkey. *Fresenius Environ. Bull.* **2017**, *26*, 520–526.
6. Rosta, I.; Doostkamian, M.; Ólafsson, H.; Ghafarian-Malamiri, H.; Zhang, H.; Taherian, A.; Sarif, M.; Gupta, R.; Monroy-Vargas, E. On the relationship between the 500 hPa height fluctuations and the atmosphere thickness over Iran and the Middle East. *TETHYS-J. Mediterr. Meteorol. Climatol.* **2019**, 3–14. [[CrossRef](#)]

7. Roustai, I.; Javadizadeh, F.; Dargahian, F.; Olafsson, H.; Shiri-Karimvandi, A.; Vahedinejad, S.H.; Doostkamian, M.; Monroy Vargas, E.R.; Asadolahi, A. Investigation of vorticity during prevalent winter precipitation in Iran. *Adv. Meteorol.* **2018**, *2018*, 1–13. [[CrossRef](#)]
8. Anderson, J.R.; Hardy, E.E.; Roach, J.T.; Witmer, R.E. *A Land Use and Land Cover Classification System for Use with Remote Sensor Data*; US Government Printing Office: Washington, DC, USA, 1976; Volume 28.
9. Gu, Y.; Brown, J.F.; Verdin, J.P.; Wardlow, B. A five-year analysis of MODIS NDVI and NDWI for grassland drought assessment over the central Great Plains of the United States. *Geophys. Res. Lett.* **2007**, *34*, 1–6. [[CrossRef](#)]
10. Reed, B.C.; Brown, J.F.; VanderZee, D.; Loveland, T.R.; Merchant, J.W.; Ohlen, D.O. Measuring phenological variability from satellite imagery. *J. Veg. Sci.* **1994**, *5*, 703–714. [[CrossRef](#)]
11. Peters, A.J.; Walter-Shea, E.A.; Ji, L.; Vina, A.; Hayes, M.; Svoboda, M.D. Drought monitoring with NDVI-based standardized vegetation index. *Photogramm. Eng. Remote Sens.* **2002**, *68*, 71–75.
12. Roustai, I.; Khosh Akhlagh, F.; Soltani, M.; Modir Taheri, S.S. Assessment of blocking effects on rainfall in northwestern Iran. In Proceedings of the COMECAP 2014, Heraklion Crete, Greece, 28–31 May 2014; Volume 291.
13. Hazaymeh, K.; Hassan, Q.K. A remote sensing-based agricultural drought indicator and its implementation over a semi-arid region, Jordan. *J. Arid Land* **2017**, *9*, 319–330. [[CrossRef](#)]
14. Cheng, C.-H.; Nnadi, F.; Liou, Y.-A. A regional land use drought index for Florida. *Remote Sens.* **2015**, *7*, 17149–17167. [[CrossRef](#)]
15. Dutta, D.; Kundu, A.; Patel, N.; Saha, S.; Siddiqui, A. Assessment of agricultural drought in Rajasthan (India) using remote sensing derived Vegetation Condition Index (VCI) and Standardized Precipitation Index (SPI). *Egypt. J. Remote Sens. Space Sci.* **2015**, *18*, 53–63. [[CrossRef](#)]
16. Liou, Y.-A.; Mulualem, G.M. Spatio-temporal Assessment of Drought in Ethiopia and the Impact of Recent Intense Droughts. *Remote Sens.* **2019**, *11*, 1828. [[CrossRef](#)]
17. AghaKouchak, A.; Farahmand, A.; Melton, F.; Teixeira, J.; Anderson, M.; Wardlow, B.D.; Hain, C. Remote sensing of drought: Progress, challenges and opportunities. *Rev. Geophys.* **2015**, *53*, 452–480. [[CrossRef](#)]
18. Zhang, X.; Wu, S.; Yan, X.; Chen, Z. A global classification of vegetation based on NDVI, rainfall and temperature. *Int. J. Climatol.* **2017**, *37*, 2318–2324. [[CrossRef](#)]
19. Gamon, J.A.; Field, C.B.; Goulden, M.L.; Griffin, K.L.; Hartley, A.E.; Joel, G.; Peñuelas, J.; Valentini, R. Relationships between NDVI, canopy structure, and photosynthesis in three Californian vegetation types. *Ecol. Appl.* **1995**, *5*, 28–41. [[CrossRef](#)]
20. Drori, R.; Dan, H.; Sprintsin, M.; Sheffer, E. Precipitation-Sensitive Dynamic Threshold: A New and Simple Method to Detect and Monitor Forest and Woody Vegetation Cover in Sub-Humid to Arid Areas. *Remote Sens.* **2020**, *12*, 1231. [[CrossRef](#)]
21. Liu, Q.; Zhang, S.; Zhang, H.; Bai, Y.; Zhang, J. Monitoring drought using composite drought indices based on remote sensing. *Sci. Total Environ.* **2020**, *711*, 134585. [[CrossRef](#)]
22. Rouse, J.; Haas, R.; Schelle, J.; Deering, D.; Harlan, J. *Monitoring the Vernal Advancement or Retrogradation of Natural Vegetation*; NASA/GSFC Type III Final Report Green-Belt MD; Texas University Press: Austin, TX, USA, 1974; Volume 371.
23. Tucker, C.J. Red and photographic infrared linear combinations for monitoring vegetation. *Remote Sens. Environ.* **1979**, *8*, 127–150. [[CrossRef](#)]
24. Chen, D.; Brutsaert, W. Satellite-sensed distribution and spatial patterns of vegetation parameters over a tallgrass prairie. *J. Atmos. Sci.* **1998**, *55*, 1225–1238. [[CrossRef](#)]
25. Gao, B.-C.; Goetz, A.F. Retrieval of equivalent water thickness and information related to biochemical components of vegetation canopies from AVIRIS data. *Remote Sens. Environ.* **1995**, *52*, 155–162. [[CrossRef](#)]
26. Kogan, F.N. Droughts of the late 1980s in the United States as derived from NOAA polar-orbiting satellite data. *Bull. Am. Meteorol. Soc.* **1995**, *76*, 655–668. [[CrossRef](#)]
27. Yang, L.; Wylie, B.K.; Tieszen, L.L.; Reed, B.C. An analysis of relationships among climate forcing and time-integrated NDVI of grasslands over the US northern and central Great Plains. *Remote Sens. Environ.* **1998**, *65*, 25–37. [[CrossRef](#)]
28. Ji, L.; Peters, A.J. Assessing vegetation response to drought in the northern Great Plains using vegetation and drought indices. *Remote Sens. Environ.* **2003**, *87*, 85–98. [[CrossRef](#)]

29. Wan, Z.; Wang, P.; Li, X. Using MODIS land surface temperature and normalized difference vegetation index products for monitoring drought in the southern Great Plains, USA. *Int. J. Remote Sens.* **2004**, *25*, 61–72. [[CrossRef](#)]
30. Ghafarian Malamiri, H.; Rousta, I.; Olafsson, H.; Zare, H.; Zhang, H. Gap-Filling of MODIS Time Series Land Surface Temperature (LST) Products Using Singular Spectrum Analysis (SSA). *Atmosphere* **2018**, *9*, 334. [[CrossRef](#)]
31. Rundquist, B.C.; Harrington, J.A., Jr. The effects of climatic factors on vegetation dynamics of tallgrass and shortgrass cover. *GeoCarto Int.* **2000**, *15*, 33–38. [[CrossRef](#)]
32. Wang, J.; Price, K.; Rich, P. Spatial patterns of NDVI in response to precipitation and temperature in the central Great Plains. *Int. J. Remote Sens.* **2001**, *22*, 3827–3844. [[CrossRef](#)]
33. Ji, L.; Peters, A.J. Lag and seasonality considerations in evaluating AVHRR NDVI response to precipitation. *Photogramm. Eng. Remote Sens.* **2005**, *71*, 1053–1061. [[CrossRef](#)]
34. Liu, W.; Kogan, F. Monitoring regional drought using the vegetation condition index. *Int. J. Remote Sens.* **1996**, *17*, 2761–2782. [[CrossRef](#)]
35. Kogan, F.; Yang, B.; Wei, G.; Zhiyuan, P.; Xianfeng, J. Modelling corn production in China using AVHRR-based vegetation health indices. *Int. J. Remote Sens.* **2005**, *26*, 2325–2336. [[CrossRef](#)]
36. Salazar, L.; Kogan, F.; Roytman, L. Using vegetation health indices and partial least squares method for estimation of corn yield. *Int. J. Remote Sens.* **2008**, *29*, 175–189. [[CrossRef](#)]
37. Martiny, N.; Camberlin, P.; Richard, Y.; Philippon, N. Compared regimes of NDVI and rainfall in semi-arid regions of Africa. *Int. J. Remote Sens.* **2006**, *27*, 5201–5223. [[CrossRef](#)]
38. Almazroui, M. Calibration of TRMM rainfall climatology over Saudi Arabia during 1998–2009. *Atmos. Res.* **2011**, *99*, 400–414. [[CrossRef](#)]
39. Islam, M.N.; Uyeda, H. Use of TRMM in determining the climatic characteristics of rainfall over Bangladesh. *Remote Sens. Environ.* **2007**, *108*, 264–276. [[CrossRef](#)]
40. Moffitt, C.B.; Hossain, F.; Adler, R.F.; Yilmaz, K.K.; Pierce, H.F. Validation of a TRMM-based global Flood Detection System in Bangladesh. *Int. J. Appl. Earth Obs. Geoinf.* **2011**, *13*, 165–177. [[CrossRef](#)]
41. Rousta, I.; Olafsson, H.; Moniruzzaman, M.; Ardö, J.; Zhang, H.; Mushore, T.D.; Shahin, S.; Azim, S. The 2000–2017 Drought risk Assessment of the Western and Southwestern Basins in Iran. *Modeling Earth Syst. Environ.* **2020**, *6*, 1201–1221. [[CrossRef](#)]
42. Du, L.; Tian, Q.; Yu, T.; Meng, Q.; Jancso, T.; Udvardy, P.; Huang, Y. A comprehensive drought monitoring method integrating MODIS and TRMM data. *Int. J. Appl. Earth Obs. Geoinf.* **2013**, *23*, 245–253. [[CrossRef](#)]
43. Parenti, C. Flower of war: An environmental history of opium poppy in Afghanistan. *SAIS Rev. Int. Aff.* **2015**, *35*, 183–200. [[CrossRef](#)]
44. Price, R. *Climate change as a driver of conflict in Afghanistan and other Fragile and Conflict Affected States*; Institute of Development Studies: Brighton, UK, 2019; Volume 18.
45. Snetkov, A. *The Regional Dimensions to Security: Other Sides of Afghanistan*; Springer: Zurich, Switzerland, 2013; Volume 273.
46. Saba, D.S. Afghanistan: Environmental degradation in a fragile ecological setting. *Int. J. Sustain. Dev. World Ecol.* **2001**, *8*, 279–289. [[CrossRef](#)]
47. Savage, M.; Dougherty, B.; Hamza, M.; Butterfield, R.; Bharwani, S. *Socio-Economic Impacts of Climate Change in Afghanistan*; Stockholm Environment Institute Press: Stockholm, Sweden, 2009; Volume 44.
48. Flohn, H. Zum Klima und Wasserhaushalt des Hindukuschs und der benachbarten Hochgebirge (The Climate and Water-Budget of the Hindu Kush and Neighbouring Mountain Ranges). *Erdkunde* **1969**, *3*, 205–215.
49. Breckle, S.-W. Flora and vegetation of Afghanistan. *Basic Appl. Dryland Res.* **2007**, *1*, 155–194. [[CrossRef](#)]
50. Rathjens, C. Die Wälder von Nuristan und Paktia. Standortbedingungen und Nutzung der ostafghanischen Waldgebiete. *Geogr. Z.* **1974**, *2*, 295–311.
51. McSweeney, C.; New, M.; Lizcano, G. UNDP climate change country profiles: Afghanistan. pp. 1–26. Available online: <https://www.geog.ox.ac.uk/research/climate/projects/undp-cp/> (accessed on 20 May 2019).
52. Kamal, G.M. *River Basins and Watersheds of Afghanistan*; Afghanistan Information Management Services (AIMS): Kabul, Afghanistan, 2004; Volume 1, pp. 1–7.
53. Akhtar, F.; Awan, U.K.; Tischbein, B.; Liaqat, U.W. Assessment of Irrigation Performance in Large River Basins under Data Scarce Environment—A Case of Kabul River Basin, Afghanistan. *Remote Sens.* **2018**, *10*, 972. [[CrossRef](#)]

54. Najmuddin, O.; Deng, X.; Siqi, J. Scenario analysis of land use change in Kabul river basin—a river basin with rapid socio-economic changes in Afghanistan. *Phys. Chem. Earth Parts A/B/C* **2017**, *101*, 121–136. [[CrossRef](#)]
55. Mack, T.J.; Chornack, M.P.; Taher, M.R. Groundwater-level trends and implications for sustainable water use in the Kabul Basin, Afghanistan. *Environ. Syst. Decis.* **2013**, *33*, 457–467. [[CrossRef](#)]
56. Rathjens, C. Fragen der horizontalen und vertikalen Landschaftsgliederung in Hochgebirgssystem des Hindykusch. *Erdwiss. Forsch.* **1972**, *4*, 205–220.
57. Favre, R.; Kamal, G.M. Watershed atlas of Afghanistan, working document for planners, parts I and II, 1st ed. Kabul: Government of Afghanistan, Ministry of Irrigation. *Water Resour. Environ.* **2004**, *60*, 1–40.
58. Zandbergen, P. Applications of shuttle radar topography mission elevation data. *Geogr. Compass* **2008**, *2*, 1404–1431. [[CrossRef](#)]
59. Gitelson, A.A.; Viña, A.; Arkebauer, T.J.; Rundquist, D.C.; Keydan, G.; Leavitt, B. Remote estimation of leaf area index and green leaf biomass in maize canopies. *Geophys. Res. Lett.* **2003**, *30*, 1–4. [[CrossRef](#)]
60. Martínez, B.; Gilabert, M.A. Vegetation dynamics from NDVI time series analysis using the wavelet transform. *Remote Sens. Environ.* **2009**, *113*, 1823–1842. [[CrossRef](#)]
61. Moulin, S.; Kergoat, L.; Viovy, N.; Dedieu, G. Global-scale assessment of vegetation phenology using NOAA/AVHRR satellite measurements. *J. Clim.* **1997**, *10*, 1154–1170. [[CrossRef](#)]
62. Mushore, T.D.; Dube, T.; Manjowe, M.; Gumindoga, W.; Chemura, A.; Rousta, I.; Odindi, J.; Mutanga, O. Remotely sensed retrieval of Local Climate Zones and their linkages to land surface temperature in Harare metropolitan city, Zimbabwe. *Urban Clim.* **2019**, *27*, 259–271. [[CrossRef](#)]
63. Running, S.W.; Loveland, T.R.; Pierce, L.L.; Nemani, R.R.; Hunt, E.R., Jr. A remote sensing based vegetation classification logic for global land cover analysis. *Remote Sens. Environ.* **1995**, *51*, 39–48. [[CrossRef](#)]
64. Broge, N.H.; Leblanc, E. Comparing prediction power and stability of broadband and hyperspectral vegetation indices for estimation of green leaf area index and canopy chlorophyll density. *Remote Sens. Environ.* **2001**, *76*, 156–172. [[CrossRef](#)]
65. Rouse, J.; Haas, R.; Schell, J.; Deering, D. Monitoring vegetation systems in the Great Plains with ERTS. *NASA Spec. Publ.* **1974**, *351*, 309.
66. Didan, K. MOD13Q1 MODIS/Terra Vegetation Indices 16-day L3 global 250 m SIN Grid V006. NASA EOSDIS Land Process. DAAC 2015. Available online: <https://lpdaac.usgs.gov/> (accessed on 12 February 2019).
67. Duan, Z.; Bastiaanssen, W. First results from Version 7 TRMM 3B43 precipitation product in combination with a new downscaling–calibration procedure. *Remote Sens. Environ.* **2013**, *131*, 1–13. [[CrossRef](#)]
68. Deng, G.; Zhang, H.; Guo, X.; Ying, H. Assessment of Drought in Democratic People’s Republic of Korea in 2017 Using TRMM Data. In Proceedings of the 2018 Fifth International Workshop on Earth Observation and Remote Sensing Applications (EORSA), Xi’an, China, 18–20 June 2018; Volume 474.
69. Kummerow, C.; Barnes, W.; Kozu, T.; Shiue, J.; Simpson, J. The tropical rainfall measuring mission (TRMM) sensor package. *J. Atmos. Ocean. Technol.* **1998**, *15*, 809–817. [[CrossRef](#)]
70. Mossad, A.; Alazba, A. Determination and prediction of standardized precipitation index (SPI) using TRMM data in arid ecosystems. *Arab. J. Geosci.* **2018**, *11*, 132. [[CrossRef](#)]
71. Nastos, P.; Kapsomenakis, J.; Philandras, K. Evaluation of the TRMM 3B43 gridded precipitation estimates over Greece. *Atmos. Res.* **2016**, *169*, 497–514. [[CrossRef](#)]
72. Huffman, G.J.; Adler, R.F.; Arkin, P.; Chang, A.; Ferraro, R.; Gruber, A.; Janowiak, J.; McNab, A.; Rudolf, B.; Schneider, U. The global precipitation climatology project (GPCP) combined precipitation dataset. *Bull. Am. Meteorol. Soc.* **1997**, *78*, 5–20. [[CrossRef](#)]
73. Huffman, G.; Stocker, E.; Bolvin, D.; Nelkin, E.; Jackson, T. GPM IMERG Final Precipitation L3 Half Hourly 0.1 Degree × 0.1 Degree V06, Greenbelt, MD, Goddard Earth Sciences Data and Information Services Center (GES DISC). 2019. Available online: <https://disc.gsfc.nasa.gov/datasets> (accessed on 12 February 2019).
74. McKee, T.B.; Doesken, N.J.; Kleist, J. The relationship of drought frequency and duration to time scales. In Proceedings of the 8th Conference on Applied Climatology, Anaheim, CA, USA, 17–22 January 1993; pp. 179–183.
75. Thom, H.C. A note on the gamma distribution. *Mon. Weather Rev.* **1958**, *86*, 117–122. [[CrossRef](#)]
76. Cancelliere, A.; Di Mauro, G.; Bonaccorso, B.; Rossi, G. Drought forecasting using the standardized precipitation index. *Water Resour. Manag.* **2007**, *21*, 801–819. [[CrossRef](#)]
77. Shah, R.; Bharadiya, N.; Manekar, V. Drought index computation using standardized precipitation index (SPI) method for Surat District, Gujarat. *Aquat. Procedia* **2015**, *4*, 1243–1249. [[CrossRef](#)]

78. Unganai, L.S.; Kogan, F.N. Drought monitoring and corn yield estimation in Southern Africa from AVHRR data. *Remote Sens. Environ.* **1998**, *63*, 219–232. [[CrossRef](#)]
79. Thenkabail, P.S.; Gamage, M. *The Use of Remote Sensing Data for Drought Assessment and Monitoring in Southwest Asia*; Iwmi: Colombo, Sri Lanka, 2004; Volume 85, p. 25.
80. Jain, S.K.; Keshri, R.; Goswami, A.; Sarkar, A.; Chaudhry, A. Identification of drought-vulnerable areas using NOAA AVHRR data. *Int. J. Remote Sens.* **2009**, *30*, 2653–2668. [[CrossRef](#)]
81. Chen, J.; Jönsson, P.; Tamura, M.; Gu, Z.; Matsushita, B.; Eklundh, L. A simple method for reconstructing a high-quality NDVI time-series data set based on the Savitzky–Golay filter. *Remote Sens. Environ.* **2004**, *91*, 332–344. [[CrossRef](#)]
82. Song, K.-B.; Baek, Y.-S.; Hong, D.H.; Jang, G. Short-term load forecasting for the holidays using fuzzy linear regression method. *IEEE Trans. Power Syst.* **2005**, *20*, 96–101. [[CrossRef](#)]
83. Pervez, M.S.; Budde, M.; Rowland, J. Mapping irrigated areas in Afghanistan over the past decade using MODIS NDVI. *Remote Sens. Environ.* **2014**, *149*, 155–165. [[CrossRef](#)]
84. Shokory, J.A.N.; Tsutsumi, J.-i.G.; Yamada, H.; Kløve, B. Intra-seasonal Variation of Rainfall and Climate Characteristics in Kabul River Basin. *Cent. Asian J. Water Res. (CAJWR) Центральноазиатский Журнал Исследований Водных Ресурсов* **2017**, *3*, 2689.



© 2020 by the authors. Licensee MDPI, Basel, Switzerland. This article is an open access article distributed under the terms and conditions of the Creative Commons Attribution (CC BY) license (<http://creativecommons.org/licenses/by/4.0/>).